Characterization of a human tooth with carious lesions using conventional and synchrotron radiation-based micro computed tomography

Iwona Dziadowiec[a], Felix Beckmann[b], Georg Schulz[a], Hans Deyhle[a], and Bert Müller[a]*
[a]Biomaterials Science Center, University of Basel, c/o University Hospital Basel, 4031 Basel, Switzerland; [b]Institute of Materials Research, Helmholtz-Zentrum Geesthacht, Max-Planck-Str. 1, 21502 Geesthacht, Germany

ABSTRACT

In a dental office, every day X rays of teeth within the oral cavity are obtained. Caries induces a mineral loss and, therefore, becomes visible by reduced X-ray absorption. The detailed spatial distribution of the mineral loss, however, is inaccessible in conventional dental radiology, since the dose for such studies is intolerable. As a consequence, such measurements can only be performed after tooth extraction. We have taken advantage of synchrotron radiation-based micro computed tomography to characterize a human tooth with a rather small, natural caries lesion and an artificially induced lesion provoked by acidic etching. Both halves of the tooth were separately visualized from 2400 radiographs recorded at the beam line P07 / PETRA III (HASYLAB at DESY, Hamburg, Germany) with an asymmetric rotation axis at photon energy of 45 keV. Because of the setup, one finds an energy shift in the horizontal plane, to be corrected. After the appropriate three-dimensional registration of the data with the ones of the same crown using the better accessible phoenix nanotom® m of General Electric, Wunstorf, Germany, one can determine the joint histogram, which enable to calibrate the system with the conventional X-ray source.

Keywords: Caries, microtomography, three-dimensional registration, joint histogram, synchrotron radiation, nanotom, photon energy, de- and re-mineralization

1. INTRODUCTION

In a dental office, every day X rays of crowns within the oral cavity are obtained. The detailed micro-morphology and spatial distribution of the mineral density, however, is inaccessible, since appropriate spatial and density resolution are only available at doses intolerable for the patients. With the higher doses found in micro computed tomography (μCT), more detailed results can be obtained [1-4]. Caries induces a mineral loss and, therefore, becomes visible by reduced X-ray attenuation. In the early stage cases, the regeneration of affected tissue can be accelerated applying short, self-assembled peptides assumed to form supra-molecular networks and trigger the nucleation of hydroxyapatite crystallites within the lesion [5, 6].

Synchrotron radiation facilities provide such high X-ray intensities that an almost monochromatic beam with tunable photon energy for micro computed tomography becomes available. Therefore, one can derive the local X-ray absorption, for example, within the hard tissue of a human crown. The availability of SRμCT, however, is restricted. As a consequence, researchers often perform μCT experiments with conventional X-ray sources. The results, especially for hard tissues, show many anatomical features with reasonable contrast [7-10]. For sure, the data have to be corrected for beam hardening and other artifacts. The question arises how far the gray values obtained by means of conventional μCT correspond to the actual X-ray absorption values at the selected, optimized photon energy. The comparison of predicted and measured X-ray absorption obtained from phantoms can support the calibration of the data [11], but are time consuming and cannot perfectly describe a wide range of tooth and bone mineralization. A deconvolution with the energy spectrum of the photons from the conventional source is also complex and generally not included.

*bert.mueller@unibas.ch; phone +41 61 265 9660; fax +41 61 265 9699; www.bmc.unibas.ch

Developments in X-Ray Tomography IX, edited by Stuart R. Stock, Proc. of SPIE Vol. 9212, 92120W · © 2014 SPIE · CCC code: 0277-786X/14/$18 · doi: 10.1117/12.2060574

We hypothesize that a joint histogram of conventional μCT with SRμCT data of the specimen of interest, here a crown of a human tooth with carious lesions, give a clear insight into the relation between determined gray values of a dedicated conventional system and the local X-ray absorption values at the selected photon energy. The validation of these quantities is of importance, for example, when investigating remineralization effects on carious lesions. The main effort corresponds to the three-dimensional registration, which includes the appropriate choice of the algorithm.

2. EXPERIMENTAL

2.1 Specimen preparation

The preparation procedures of the specimen, a crown of a human tooth, were conducted in agreement with the Declaration of Helsinki and according to the ethical guidelines of the Canton of Basel, Switzerland. The approval of the study protocol got the number 290/13 from the responsible Swiss ethical committee. The tooth was extracted for clinical reasons unrelated to the study. The donated tooth crown with a small carious lesion was anonymized. The volume of the inspected portion of the crown corresponds to approximately 0.3 cm^3.

2.2 Synchrotron radiation-based micro computed tomography

The three-dimensional image of the crown of the tooth was obtained from 2400 radiographs with a pixel size of 4.8 μm, recorded at the beamline P07 operated by HZG at the storage ring PETRA III (DESY, Hamburg, Germany). For applying high-density resolution microtomography we optimize the beamline for the use of a high-flux monochromatic X-ray beam at the photon energy of about 45 keV [12]. The main components affecting the spectrum and the photon flux at the beamline are the undulator installed in the PETRA III storage ring, the double-crystal bent-Laue monochromator (Si(111)) and attenuating components (e.g. filter, Si-crystal, beam pipe, air) within the beam path. The basic design of the monochromator was optimized for the operation of diffraction experiments using a field-of-view of only 1 × 1 mm² with the photon energy range of 50 – 200 keV. The water/cooled double crystal monochromator uses Si(111) crystals in horizontal Laue scattering geometry (thickness 1.25 mm, asymmetric cut of 35.36°). For the optimization of the transmitted bandwidth the crystals are bent in Rowland geometry. The beamline is normally operated in high-beta mode resulting in a field-of-view at the tomography experiment of 2 × 2 mm². For imaging application, which requires a larger field-of-view the beamline is operated in low-beta mode for the use of the full width of the undulator spectrum and a field-of-view at the tomography experiment of about 7 × 2 mm². To increase the photon flux an evacuated pipe is installed to suppress the attenuation of 37 m air path between the monochromator and the experiment.

Due to the bending of the monochromator crystals, one may find a shift of the photon energy in the horizontal plane of the X-ray beam. This can only be avoided, if the bending is carefully aligned to a radius of about 39.5 m. The alignment of the bending of the crystals is time consuming and, therefore, only be done and tested during commissioning shifts. Normally, it is optimized for the selected photon energy. Especially for imaging applications the used photon energy is selected for the optimal transmission of the investigated specimen. Without going into too much detail we calculate the X-ray spectrum and intensity for the used setup for the presented measurement. The influence of the installed components to the X-ray spectrum is shown in the diagrams of Figure 1.

The measurements did not indicate any detectable energy shift along the beam profile from crystal bending. There was no artifact within the reconstructed data.

The crown was rotated with equi-angular steps between 0 and 360° with an asymmetric rotation axis. This approach allows for a spatial resolution, which is up to a factor of two larger than the conventional approach with a rotation axis in the center of the specimen [13]. As the height of the specimen exceeds the one of the monochromatic X-ray beam, we have recorded radiographs for tomograms in 2 vertical steps. In Figure 2 a 3D rendering represents the total reconstructed volume of one of the two halves of the human crown. Experts can easily identify the carious lesions visible by the reduced attenuation (gray).

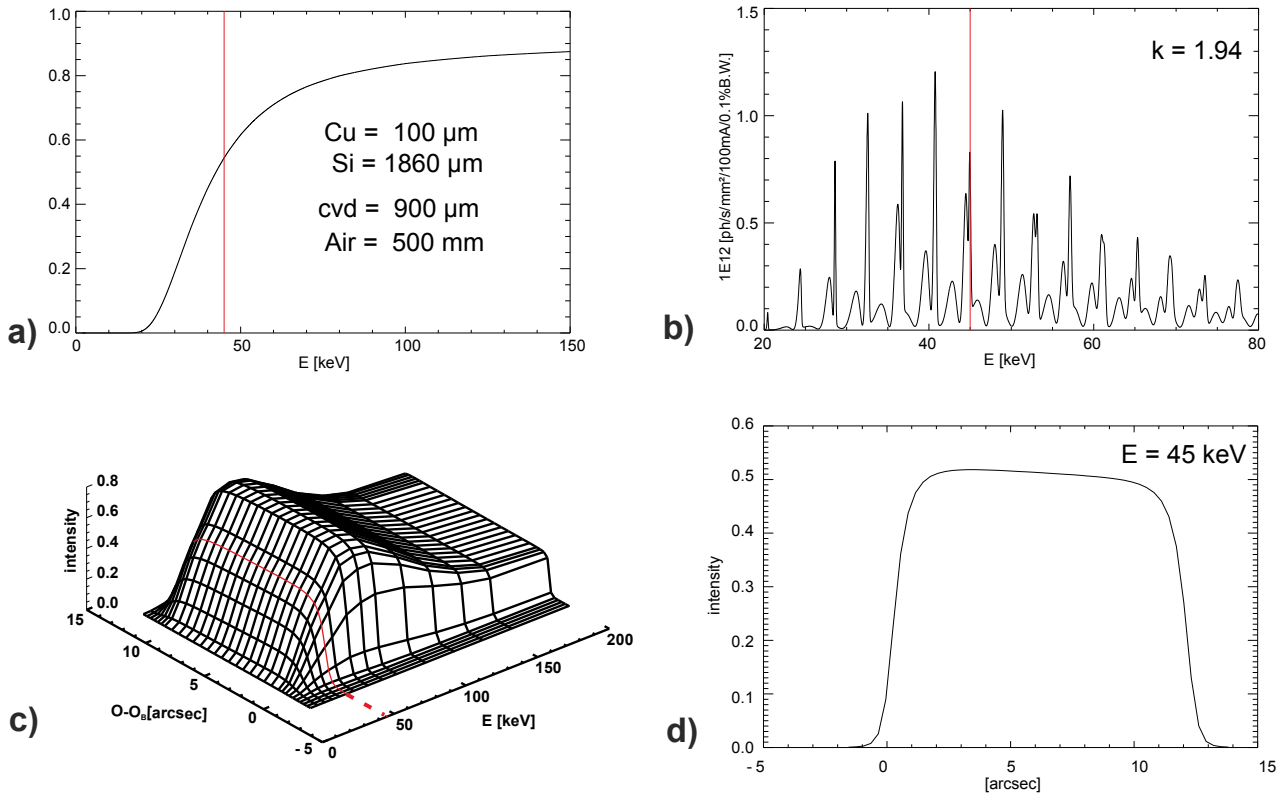

Figure 1. Experimental parameters for using a photon energy of 45 keV (marked in red) at beamline P07 / PETRA III (DESY, Hamburg, Germany). a) Attenuation with respect to the photon energy of the installed components at the beamline P07 except double crystal monochromator. The total thickness of the attenuating material is given. b) Intensity profile at the sample position for the used undulator gap including the attenuation of the installed components. c) Intensity of the double crystal bend-Laue monochromator with respect to photon energy (Si(111)). The calculation of the spectrum is done for the optimal bending (R = 39.5 m). d) Intensity profile of the double crystal monochromator for 45 keV. The calculation of the plots was done using IDL, XOP, and SPECTRA [http://www.exelisvis.com/ProductsServices/IDL.aspx, http://www.esrf.eu/Instrumentation/software/data-analysis/xop2.3/download, http://radiant.spring8.or.jp/spectra/spectra_download.html].

2.3 Conventional micro computed tomography

Micro computed tomography data of the same crown were subsequently measured at the University of Basel using the better accessible phoenix nanotom® m of General Electric, Wunstorf, Germany. 1200 equiangular projections were acquired over 360° at an acceleration voltage of 90 kV. A 2 mm-thin Cu filter was used to intentionally harden the X-ray spectrum from the nanofocus transmission tungsten tube. The pixel size of the recorded and reconstructed data corresponded to 4.8 µm.

2.4 Three-dimensional registration of tomography data

The tomography data of the conventional and the synchrotron radiation-based micro computed tomography were rigidly registered [14]. The dataset from the conventional X-ray source served as reference, whereas the three-dimensional data of the, beamline P07, as the so-called floating data, were shifted, rotated, and interpolated in three-dimensional space to optimized fit the reference. For ease of handling and improved density resolution, the data were binned by a factor of four before registration.

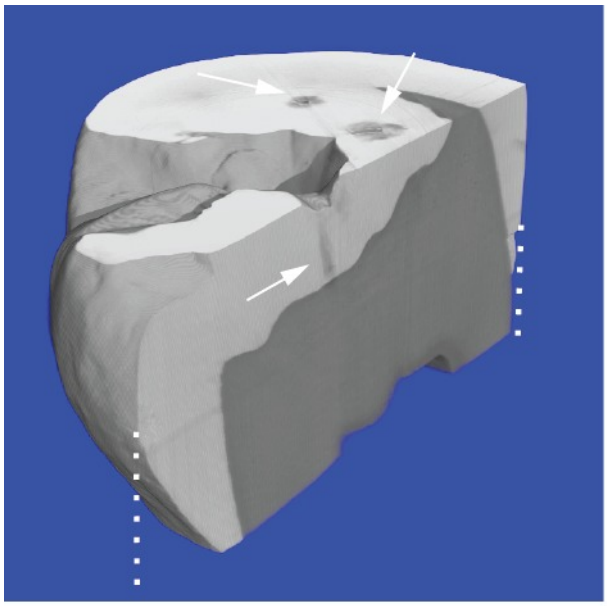

Figure 2. 3D rendering of the SRμCT data acquired at the beamline P07 / PETRA III (Hamburg, Germany) using a photon energy of 45 keV. The distance between the marked lines is 9 mm. The carious lesions within the enamel can clearly be seen by darker gray, and are indicated by arrows.

3. RESULTS AND DISCUSSION

Synchrotron radiation-based micro computed tomography data are known not only to provide local X-ray absorption values of the specimen but also to lead to three-dimensional images of high contrast [15]. Conventional micro computed tomography is also well established to visualize hard tissues with superior spatial and density resolutions [8-10]. As a consequence, the differences are expected to be rather small. Figure 3 displays the corresponding slices obtained from the two facilities after three-dimensional registration. One has difficulties to identify the differences between the slices. On a first glance, the marginal differences are assumed to originate from the registration and related interpolation of the registered dataset.

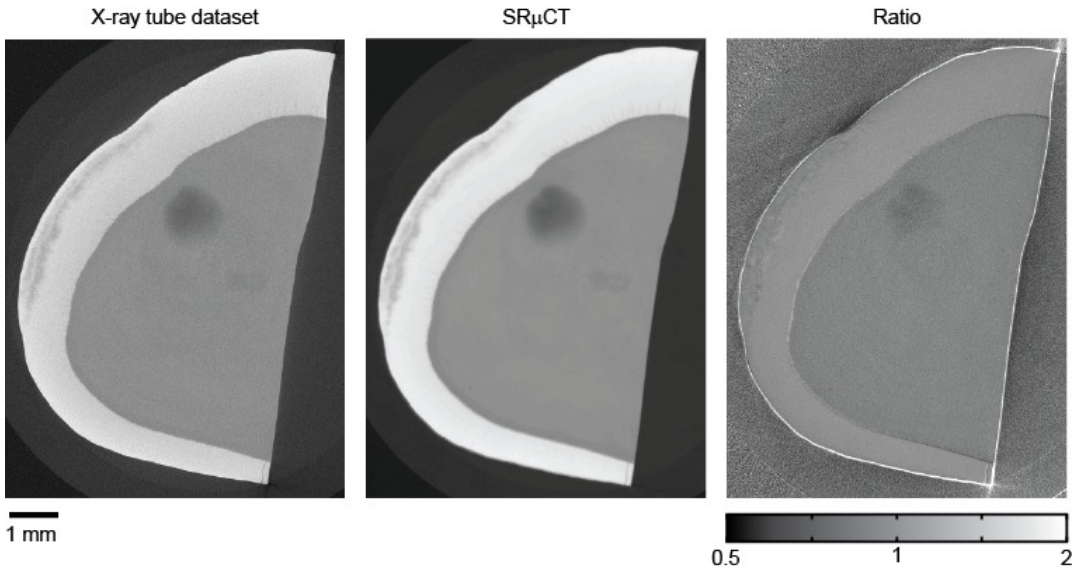

Figure 3. As known from highly mineralized human tissues, the differences in images from conventional and synchrotron radiation-based systems are hardly seen. The rightmost image shows the ratio of the X-ray tube over the SRμCT dataset. Both enamel and dentin appear homogeneous.

The selected slice of Figure 3 exhibits the characteristic anatomical features. The part of strongest absorption is enamel in health. Within the enamel one recognizes an area of reduced absorption (darker gray), which corresponds to the caries lesion. The lesion exhibits the characteristic shape captured by a higher mineralized membrane-like top-layer, with underlying stratified regions of higher and lesser demineralization [16]. The dentin shows a degree of mineralization that is similar to that of the lesion. The even less absorbing circularly shaped part is carious dentin.

The point-wise ratio (X-ray tube over SRμCT) of the two datasets (cf. Figure 3, right) reveals slight differences between the datasets. The white border of 1-2 pixels (20-30 μm) width, surrounding the specimen, results from a minimal mismatch in pixel dimensions. Since the specimen and the features of interest within are one to two orders of magnitude larger, this mismatch is still reasonably small. Otherwise, no significant distortions in specimen shape were found. Enamel, dentin, and the carious lesions within both enamel and dentin can be identified. Note, the ratio of higher absorbing regions is higher that that of lower absorbing material. As can be seen in Figures 4 and 5, the relation between attenuation from lab-source and synchrotron is almost linear. The different ratio values derive from a proportionality factor that differs from unity.

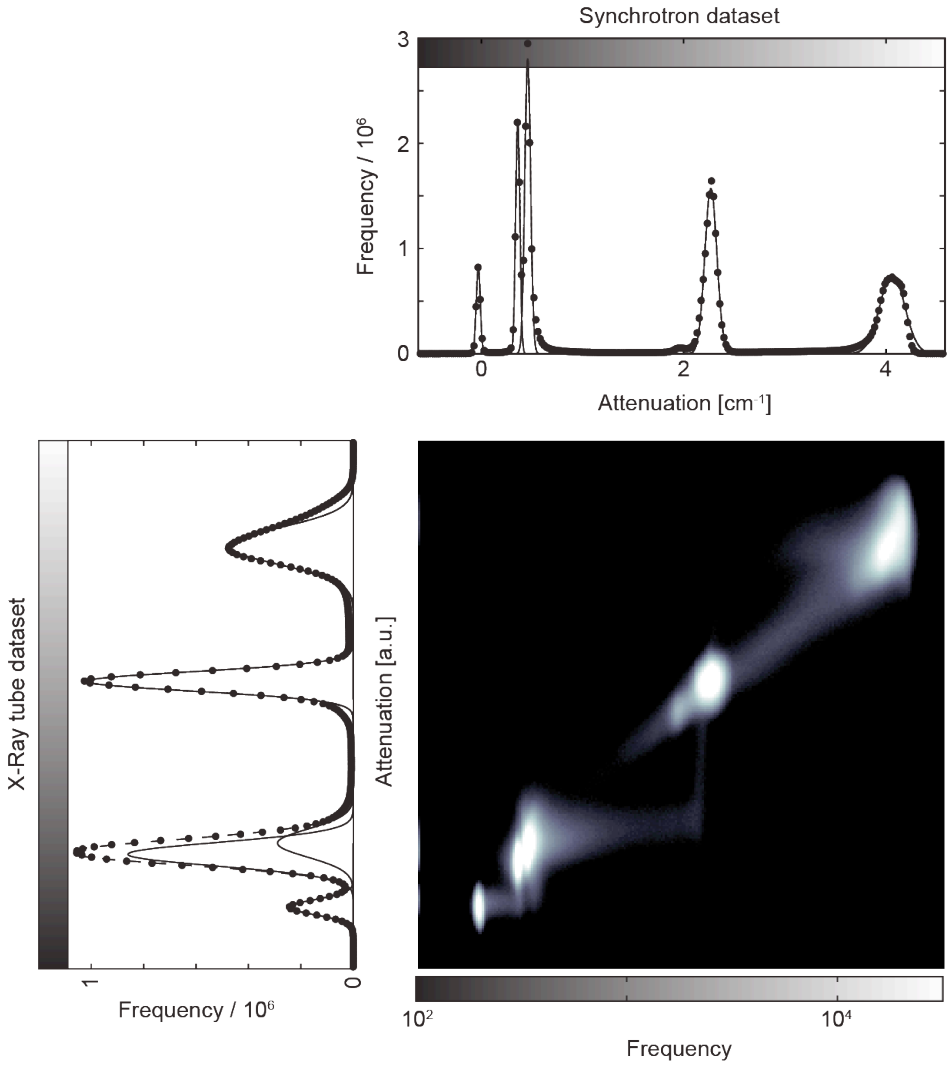

Figure 4. The registered three-dimensional data of conventional and synchrotron radiation-based tomography can be represented by a joint histogram. Each count in this gray-scale image corresponds to one voxel in each tomogram. Integration along the x- and y-axis, respectively, gives rise to the histogram of the X-ray absorption in the individual data. If the data are identical, one finds a line in the histogram with a broadening according to the photon statistics. The deviation from a line is rather small. The main peaks in both the X-ray tube and SRμCT histograms were fitted with Gaussians.

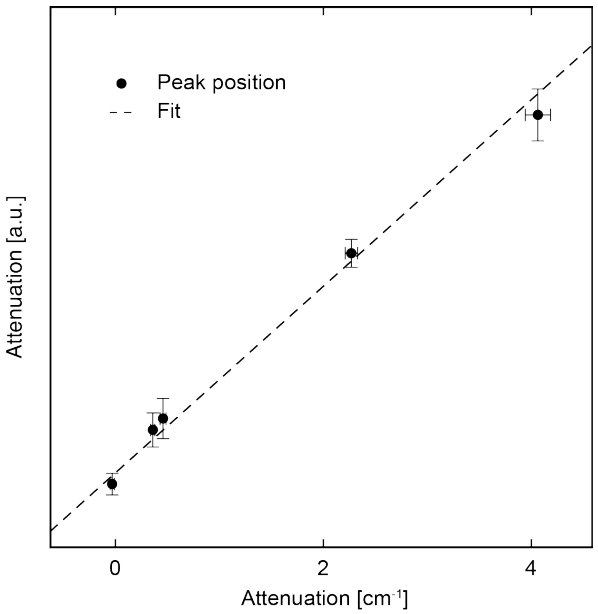

Figure 5. The peak position of the SRμCT (abscissa) and X-ray tube (ordinate) data can be plotted against each other. Attenuation values from both methods scale almost linearly (correlation coefficient 0.9972). The error bars correspond to the standard deviation of the Gaussians.

Figure 4 (top and bottom left) shows the histograms of the SRμCT and X-ray tube datasets, respectively. For both datasets, one can identify distinct peaks corresponding to air, container/water, enamel and dentin (from lowest to highest absorption values), which can be fitted using Gaussians. Due to the small volume of the carious regions, these give rise to shoulders in the peaks corresponding to enamel and dentin. Despite the similarity of the data, the higher density resolution of the SRμCT becomes evident through the sharper peaks.

Since the attenuation values obtained from X-ray tube sources depend on various factors such as anode material, filters used, beam hardening, or eventual corrections during reconstruction, these values are of a more qualitative nature. It is also unclear whether they depend linearly on material density, as is the case for monochromatic X-rays. Therefore, calibration measurements, e.g. with phantoms, are often used when investigating density variations with lab source μCT [17-19].

The relation between the attenuation values obtained from SRμCT and conventional laboratory source can be further investigated by generating a joint histogram of the two datasets [14, 20]. Here, for each voxel the attenuation values from both methods are plotted against each other and the frequency of recurring values counted (cf. Figure 4). The integration of the joint histogram along each dimension yields the histograms of the individual datasets. If a linear relationship between the attenuation values is given, one finds a line in the joint histogram, with a broadening related to the photon statistics. Horizontal and vertical streaks in the gray value image are caused by surface effects due to imperfect data registration.

To assess the relationship between the attenuation values from SRμCT, the peak positions within the histograms of the two methods, obtained from the Gaussian fits, were plotted against each other (cf. Figure 5). The error bars correspond to the standard deviation of the Gaussians. Since the conventional lab source measurements yield gray values, an arbitrary scaling was chosen. An almost linear relationship between the absorption values can be seen, indicating that the chosen settings for the laboratory source measurements are appropriate.

4. CONCLUSION

Conventional micro computed tomography is a well-established technique to visualize hard tissues with superior spatial and density resolutions. However, since X-ray tube measurements generally only provide mean attenuation or even gray values, particular care has to be taken when analyzing these data concerning material density. Through the calibration with quantitative SRμCT, one can assess the relationship between gray values and X-ray attenuation for given settings, and thus validate the results in a quantitative manner.

ACKNOWLEDGEMENTS

The support of team from the Institute for Chemistry and Bioanalytics, University of Applied Sciences and Arts, Northwestern Switzerland, Basel, Switzerland for the tooth preparation is gratefully acknowledged. The project is financially supported by the Swiss National Science Foundation via the grant #51NF40-144617. The authors thank the Swiss National Science Foundation for financial support of the phoenix nanotom® m within the R'Equip initiative (grant 316030_133802/1).

REFERENCES

[1] Dowker, S.E.P., Elliot, J.C., Davis, G.R*., et al.*, "Longitudinal Study of the Three-Dimensional Development of Subsurface Enamel Lesions during in vitro Demineralisation," Caries Research **37**, 237-245 (2002).

[2] Fearne, J., Anderson, P., and Davis, G.R., "3D X-ray microscopic study of the extent of variations in enamel density in first permanent molars with idiopathic enamel hypomineralisation," British Dental Journal **196**, 634-638 (2004).

[3] Wong, F.S.L., Anderson, P., Fan, H*., et al.*, "X-ray microtomographic study of mineral concentration distribution in deciduous enamel," Archives of Oral Biology **49**, 937-944 (2004).

[4] Delbem, A.C.B., Sassaki, K.T., Vieira, A.E.M*., et al.*, "Comparison of methods for evaluating mineral loss: Hardness versus synchrotron microcomputed tomography," Caries Research **43**, 359-365 (2009).

[5] Firth, A., Aggeli, A., Burke, J.L*., et al.*, "Biomimetic self-assembling peptides as injectable scaffolds for hard tissue engineering," Nanomed. **1** (2), 189-199 (2006).

[6] Kirkham, J., Firth, A., Vernals, D*., et al.*, "Self-assembling peptide scaffolds promote enamel remineralization," J. Dent. Res. **86** (5), 426-430 (2007).

[7] Luckow, M., Deyhle, H., Beckmann, F*., et al.*, "Tilting the jaw to improve the image quality or to reduce the dose in cone-beam computed tomography," Eur. J. Radiol. **80**, 389-393 (2011).

[8] Kühl, S., Deyhle, H., Zimmerli, M*., et al.*, "Cracks in dentin and enamel after cryo-preservation," Oral Surgery Oral Medicine Oral Pathology Oral Radiology and Endodontology **113**, 5-10 (2011).

[9] Ruegsegger, P., Koller, B., and Müller, R., "A microtomographic system for the nondestructive evaluation of bone architecture," Calcified Tissue International **58** (1), 24-29 (1996).

[10] Stock, S.R., "X-ray microtomography of materials," Int. Mater. Rev. **44** (4), 141.164 (1999).

[11] Schneider, U., Pedroni, E., and Lomax, A., "The calibration of CT Hounsfield units for radiotherapy treatment planning," Phys. Med. Biol. **41**, 111-124 (1996).

[12] Beckmann, F., Herzen, J., Haibel, A*., et al.*, "High density resolution in synchrotron-radiation-based attenuation-contrast microtomography," Proc. SPIE **7078**, 70781D (2008).

[13] Müller, B., Bernhardt, R., Weitkamp, T*., et al.*, "Morphology of bony tissues and implants uncovered by high-resolution tomographic imaging," Int. J. Mater. Res. **98** (7), 613-621 (2007).

[14] Müller, B., Deyhle, H., Lang, S*., et al.*, "Three-dimensional registration of tomography data for quantification in biomaterials science," Int. J. Mater. Res. **103** (2), 242-249 (2012).

[15] Thurner, P., Beckmann, F., and Müller, B., "An optimization procedure for spatial and density resolution in hard X-ray micro-computed tomography," Nucl. Instrum. Meth. B **225** (4), 599-603 (2004).

[16] Gustafson, G., "The histopathology of caries of human dental enamel with special reference to the division of the carious lesion into zones," Acta. Odontol. Scand. **15**, 13-55 (1957).

[17] Huang, T.T.Y., Jones, A.S., Hong He, L*., et al.*, "Characterisation of enamel white spot lesions using X-ray micro-tomography," Journal of Dentistry **35**, 737-743 (2007).

[18] Schwass, D.R., Swain, M.V., Purton, D.G*., et al.*, " A system of salibrating microtomography for use in caries research," Caries Research **43**, 314-321 (2009).

[19] Burghardt, A.J., Kazakia, G.J., Laib, A*., et al.*, "Quantitative assessment of bone tissue mineralization with polychromatic micro-computed tomography," Calcified Tissue International **83**, 129-138 (2008).

[20] Schulz, G., Waschkies, C., Pfeiffer, F*., et al.*, "Multimodal imaging of human cerebellum - merging X-ray phase microtomography, magnetic resonance microscopy and histology," Sci. Rep. **2**, 826 (2012).